The final publication is available at

http://dx.doi.org/10.1016/j.ceramint.2017.07.072

Additional Information

Compressive strength and microstructure of alkali-activated mortars with high ceramic waste content

L. Reig[1], M.A. Sanz[2], M.V. Borrachero[2], J. Monzó[2], L. Soriano[2], J. Payá[2],

[1] Universitat Jaume I, Department of Mechanical Engineering and Construction, Castelló de la Plana, Spain; lreig@uji.es

[2] Universitat Politècnica de València, Instituto de Ciencia y Tecnología del Hormigón (ICITECH), Valencia, Spain; jjpaya@cst.upv.es, misanpar@aaa.upv.es, vborrachero@cst.upv.es, jmmonzo@cst.upv.es, lousomar@upvnet.upv.es

* Corresponding author: L. Reig, lreig@uji.es, Phone: +34 964 729161; Fax: +34 964 728106

Abstract

The present work investigated alkali-activated mortars with high ceramic waste contents. Tile ceramic waste (TCW) was used as both a recycled aggregate (TCWA) and a precursor (TCWP) to obtain a binding matrix by the alkali-activation process. Mortars with natural siliceous (quartz) and calcareous (limestone) aggregates, and with other ceramic waste materials (red clay brick RCB and ceramic sanitaryware CSW waste), were also prepared for comparison purposes. Given the lower density and higher water absorption values of the ceramic aggregates, compared to the natural ones, it was necessary to adapt the preparation process of the recycled mortars by presaturating the aggregate with water before mixing with the TCWP alkali-activated paste. Aggregate type considerably determined the mechanical behaviour of the samples cured at 65ºC for 3 days. The mortars prepared with the siliceous aggregate presented poor mechanical properties, even when cured at 65ºC. The behaviour of the limestone aggregate mortars depended heavily on the applied curing temperature and, although they presented the best mechanical properties of all those cured at room temperature, their compressive strength

1

reached a maximum when cured at 65ºC, and then decreased. The mechanical properties of the mortars prepared with TCWA progressively increased with curing time (53 MPa at 65ºC for 28 days). An optimum 50 wt.% proportion was observed for the limestone/TCWA mortars (≈43 MPa, 3 days at 65ºC), whereas the mechanical properties of that prepared with siliceous particles (10 MPa) progressively increased with the TCWA content, up to 100 wt.% substitution (23 MPa). Limestone particles interacted with the binding matrix, and played an interesting beneficial role at the 20ºC curing temperature, with a slight reduction when cured long term (28 days) at 65ºC. The results demonstrated a potential added value for these ceramic waste materials.

1 Introduction

Portland cement (PC) manufacturing is an energy-intensive process that requires high temperatures (1,450-1,550ºC), consumes natural resources (mainly limestone and clay) and generates vast greenhouse gas emissions to the atmosphere (approximately 1 ton of CO_2 per ton of produced cement. As reported in [1], it is one of the primary causes of global warming, and accounts for 7% of worldwide CO_2 emissions. As highlighted by Pachecho-Torgal [2], global warming will lead to not only increasingly extreme atmospheric events, but also to the thawing of the world's permanently frozen ground, and thermal expansion of water, both of which will result in a rising sea level.

These problems have encouraged the scientific community and cement industry to seek alternatives to reduce the energy consumed during PC production, and to develop alternative binders with lower environmental costs. Among the low CO_2 binders that are being investigated (calcium sulphoaluminate, alkali-activated materials, hybrid alkaline cements, etc.) [3], those developed by alkali-activation have allowed the reuse of a wide variety of industrial by-products as precursors to develop binding matrices. Mellado et al. [4] compared the CO_2 emissions of alkali-activated fluid catalytic cracking catalyst (FCC) waste mortars developed with commercial waterglass and sodium hydroxide solutions with those activated with an alternative active silica source (to substitute commercial waterglass). Although these authors concluded that the most important parameter to contribute to CO_2 emissions in geopolymeric mortars is the synthesis of commercial waterglass, mortars prepared with commercial solutions still reduce CO_2 emissions by 13% compared to PC mortars. As pointed out by Behera et al. [5], the alkali-activation of industrial waste also helps minimise the exploitation of non-renewable raw materials, and to reduce pollution, energy consumption and the areas employed to dispose waste, all of which help mitigate global warming.

As reviewed by Payá et al. [6] different industrial waste types have been successfully used by the scientific community to develop alternative binders by alkali activation. Ground granulated

blast furnace slag, metakaolin and fly ash are among the most widely used [6-8], and others like fluid catalytic cracking catalyst (FCC) waste [6], sugarcane bagasse ash [8], ceramic products (bricks, tiles, etc.) [9,10], or different types of glass [6], have also proved successful.

Industrial waste may also be used as recycled aggregate. As indicated by Behera et al. [5] and Silva et al. [11], the quality, quantity, size and type of recycled aggregates to be used need to be precisely characterised because they strongly influence the mechanical properties and durability of the concrete being designed. As observed by Elchalakani and Elgaali [12], recycled concrete strength is greatly influenced by the quality of aggregates. This conclusion has been corroborated in different studies where ceramic waste has been used as recycled aggregate in PC systems. Mechanical properties diminished, compared with the reference concrete, in the research by Alves et al. [13], who used fine ceramic aggregates. Medina et al. [14] reported improved mechanical properties in concrete made with recycled aggregate from ceramic sanitaryware (CSW). Among the different waste materials used as aggregates, special attention must be paid to construction and demolition waste (CDW) as it generates vast volumes of waste. According to the data reported in [2], it is estimated that 970 million tons of CDW are generated yearly in Europe, and approximately 140 million tons are produced in the US. Similarly according to [15], the average annual production of CDW generated in Spain was 15.89 tons for the 2009-2013 period. A specific CDW type is ceramic tiles, which are manufactured in large amounts in eastern Spain, which was the study area of the present work. According to the data provided by the Spanish Association of Ceramic Tile and Pavement Manufacturers (ASCER), 85.63% of the 167 Spanish companies registered in year 2013 that produced ceramic tiles and related products were located in the provinces of Valencia and Castellón (E Spain). As reported by Stock [16], the Spanish industry made 420 of the 11,913 million m^2 of tiles produced in 2013, is the fifth top manufacturing country (after China, Brazil, India and Iran) and accounts for 3.5% of world production. Thus investigating the potential use of large amounts of tile ceramic waste (TCW) in alkali-activated mortars as both a precursor and recycled aggregate is an interesting and attractive option for tile and cement industries both interested in recycling and producing sustainable materials.

The objective of this study was to develop mortars with high ceramic waste contents provided by ceramic tiles companies. This TCW was used as a recycled aggregate (sand) and also as a precursor to produce the binding matrix by the alkali-activation process. TCW was physically and chemically characterised, and the evolution of the mechanical properties and the developed microstructure were analysed in mortars cured at room temperature and at 65ºC. The compressive strength of the TCW recycled mortars was compared with that presented by the mortars that contained natural aggregates (limestone and quartz) and those prepared with other ceramic aggregate types (brick and sanitaryware waste-derived sand). Mortars that combined different proportions of natural/TCW aggregates were also investigated.

2   Materials and methods

2.1 Experimental Flow Chart

Alkali-activated tile ceramic waste mortars (TCW) were developed using natural and recycled aggregates. The TCW used herein is presented in Figure 1, and was provided by some tile manufacturing companies located in the province of Castellón (east Spain). Most particles had a diameter that fell within the 4-16 mm range. Waste was used to obtain the binder for the alkali-activation process (TCWP, as a powdered material), and as a recycled aggregate (TCWA, as a granulated material) in the developed mortars.

INSERT FIGURE 1

Siliceous (quartz) and limestone sands were used as natural aggregates, and mortars with different proportions of the natural/TCWA aggregates were prepared to assess the evolution of the mechanical properties depending on the aggregates mixture. Other ceramic materials, such as red clay brick (RCB) and ceramic sanitaryware (CSW) waste, were also used as recycled aggregates for comparison purposes. The experimental process that we followed is described in Figure 2. A further description of the different process steps is provided in Sections 2.2 to 2.5.

INSERT FIGURE 2

2.2 Preparation and characterisation of tile ceramic waste powder

The TCW powder (TCWP, as a precursor or binder) for the alkali-activation process was prepared by crushing original particles to less than 2 mm in a jaw crusher (BB200 model, Retsch) and then grinding in a jars turner roller (Gabrielli Roller 1). Grinding was achieved by turning two cylindrical alumina 5-litre volume jars for 6 h (190 rpm for the first 10 minutes and 140 rpm for the remaining time). Each jar was filled with 1,500 g of ceramic waste and 6,500 g of alumina balls. As shown in Figure 3, both the crushed particles before milling (Fig. 3a, optical microscopy) and the milled TCWP particles (Fig. 3b, SEM–EDX, JEOL JSM-6300) exhibited irregular shapes with sharp edges.

INSERT FIGURE 3

The particle size distribution of TCWP was analysed by laser diffraction in a Mastersizer 2000 (Malvern Instruments). This powder had a mean particle diameter of 28.3 µm with 90%.vol of particles (d_{90}) under 69.7 µm. As previously reported in [17], where this powder was used to produce pozzolanic cement, TCWP contained high levels of SiO_2 and Al_2O_3 (61.22 wt.% and 18.60 wt.%, respectively), together with moderate amounts of CaO (5.77 wt.%), Fe_2O_3 (5.02 wt.%) and K_2O (3.33 wt.%). The amorphous content reported in [17] for this ceramic waste was 60 wt.%, with quartz (SiO_2) in the major crystalline phase, and with mullite ($Al_6Si_2O_{13}$), albite ($NaAlSi_3O_8$), and diopside (a calcium and magnesium silicate, $CaMg(SiO_3)_2$) as minor constituents.

2.3 Preparation and characterisation of aggregates.

The as-received TCW was dried in a stove at 105±1°C for 48 h and was then crushed in a jaw crusher (BB200, Retsch) with a 4-mm opening to obtain the TCW4 aggregate. Another granulometric fraction of TCW was prepared by sieving the ceramic waste material through a 2-mm opening (TCW2). Siliceous and limestone natural aggregates were used for comparison purposes. The limestone aggregate was used as received, and had a maximum particle diameter of 4 mm. Three different siliceous aggregates were combined to obtain a new one with a similar particle size distribution to that presented by the recycled TCW2 aggregate. Two different ceramic waste materials were also used as recycled aggregates to investigate the influence of ceramic material type on the mechanical properties of the developed mortars. Thus two granulometric fractions of the RCB waste (RCB2, RCB4) and the CSW waste (CSW2, CSW4) were prepared following the same process as that described for TCWA. The particle size distribution of both the natural and recycled aggregates was determined by a sieve analysis according to UNE-EN 933-1.

The water absorption and different densities of the natural and TCW aggregates were also determined to investigate their behaviour when used in mortar samples. The loose bulk density of aggregates and the percentage of voids between particles were determined according to UNE-EN 1097-3. Then the specific density and water absorption of particles were analysed following UNE-EN 1097-7 (pyknometer test). The relative volume (V_r) of particles, which is that occupied by the solid material, plus the non-accessible voids of individual particles (Table 1), was evaluated using dry material. Relative density (ρ_r) was determined as the ratio between the weight of the dry material (W_{DRY}) and the relative volume of particles (V_r). The mass of saturated particles (W_{SAT}) was used to determine their apparent volume (V_A) (Table 1). The specific densities of the saturated ($\rho_{S\_SAT}=W_{SAT}/V_A$) and dry particles ($\rho_{S\_DRY}=W_{DRY}/V_A$) were also calculated. The described densities, together with the volumes considered and the formulae, are summarised in Table 1.

Table 1. Physical properties of the ceramic waste aggregates

	Loose bulk density and voids, g/m³, %	Relative density dry particles, g/m³	Specific density saturated particles, g/m³	Specific density dry particles, g/m³
Volume considered	V	V_r	V_A	V_A
Specification	UNE-EN 1097-3	UNE-EN 1097-7	UNE-EN 1097-7	UNE-EN 1097-7
Formulae	$\rho_L = \dfrac{W}{V}$	$\rho_r = \dfrac{W_{DRY}}{V_r}$	$\rho_{S\_SAT} = \dfrac{W_{SAT}}{V_A}$	$\rho_{S\_DRY} = \dfrac{W_{DRY}}{V_A}$

2.4 Preparing mortar samples and characterisation

The proportions and ratios of the alkali-activating solutions are summarised in Table 2. They were adapted from previous studies in which alkali-activated porcelain stoneware mortars were developed [11]. NaOH pellets (98% purity, Panreac), water and sodium silicate (Merck, SiO_2=28%, Na_2O=8%, H_2O=64%) were used for the activating solution. The binder was composed of TCWP and 5 wt.% of calcium hydroxide (93% purity) which, as described in [11], was used in all the prepared samples to activate the binding process and to favour setting and hardening. A water/binder (w/b) ratio of 0.45 was used, where water was provided by the sodium silicate reagent solution and that directly added to the activating solution.

Table 2. Mix proportions for the alkali-activated TCW mortars

Designation	w/b	$[Na^+]$, mol kg⁻¹	$[SiO_2]$, mol kg⁻¹	SiO_2/Na_2O, Molar ratio	$Ca(OH)_2$, %	Na^+, Mol kg$_{binder}$⁻¹	SiO_2, Mol kg$_{binder}$⁻¹
45/10/1.16-5	0.45	10	5.82	1.16	5	4.50	2.62

$Ca(OH)_2$ and TCWP were dry-mixed, and alkali-activated mortar samples were prepared by mixing the powder with the activating solution and adding aggregates. A binder-to-aggregate weight ratio of 1:3 was used and different mortars were prepared depending on the material used as the aggregate (TCWA, limestone sand, siliceous sand, crushed brick and crushed

sanitary ware), particle size (maximum size 2 mm or 4 mm) and the percentage of the substitution of natural aggregates for ceramic aggregates (TCWA 0 to 100 wt.%; RCB and CSW 100 wt.%). The mortar samples were placed into 4x4x16 cm^3 moulds and were vibrated to remove air bubbles. Samples were cured at 20ºC with a relative humidity (RH) of 95% for 7, 28 and 90 days, and at 65ºC (inside a sealed box, floating in a water bath) for 3, 7 and 28 days. All the samples (both those cured at 20 ºC and those at 65 ºC) were wrapped with plastic film to maintain moisture and to prevent efflorescence formation during the curing process. The compressive strengths of the developed mortars were tested according to UNE EN 196-1, and the microstructure was examined by SEM–EDX (JEOL JSM6300) and optical microscopy (LEICA MZ APO). Dissolution of aggregates was investigated by SEM analyses by comparing the original surface with that observed after immersion in the alkali-activating solution for 7 days at 65ºC. The efflorescences that arose in some developed mortars were analysed by X-ray diffraction tests (XRD, Brucker AXS D8 Advance, 5 to 70 2θ degrees, Cu Kα radiation at 40 kV and 20 mA).

3   Results

3.1 Particle size distribution of natural and recycled aggregates.

The particle size distributions of the natural (limestone and siliceous sands) and TCWA recycled aggregates (TCW2 and TCW4), together with the fineness grading modulus (FM, in parentheses), are presented in Figure 4. The limestone aggregate, which was used as received, presented a finer granulometric distribution (FM=3.92) compared to the recycled TCW4 (FM=4.44). Although the FM of the siliceous aggregate (3.28), which was prepared by combining three different granulometric fractions, was similar to that of the recycled TCW2 (3.10), the latter presented a higher percentage of fine particles (size < 0.5 mm). This is due to the crushing process of the TCW, which yielded very fine particles. These small differences between particle size distribution and the FM values of the tested aggregates may slightly influence the mechanical properties of the developed mortars due to grain packing effects.

INSERT FIGURE 4

The granulometric distribution and fineness grading modulus (FM) of the RCB waste (RCB2, RCB4) and the CSW aggregates (CSW2, CSW4) are presented in Figure 5. Although both materials were prepared following the same crushing process, the aggregates obtained from red clay hollow bricks presented the finest and coarsest distributions, as the curves and FM values indicate.

INSERT FIGURE 5

3.2 Physical properties of natural and recycled aggregates

Table 3 summarises the physical properties of the natural and recycled aggregates used in this study. Higher loose bulk density values were obtained for the natural aggregates than with the recycled ones, no matter what particle size was. This indicates less mass of recycled particles per unit volume. The high percentage of voids between particles ($\approx$ 36-48%) was attributed to the irregularly shaped aggregates, which hinders their compaction when no pressure or vibration is applied. As expected, the relative density (ρ_r) of the dry particles was higher than their specific density (ρ_{S_DRY}) since the former considers the relative volume of individual particles (solid material, plus that of the non-accessible voids within particles), while the latter is calculated with the apparent volume of individual particles (Table 1). The differences between both values (ρ_r and ρ_{S_DRY}) were more marked in the tile (TCW2 and TCW4) and brick (RCB2 and RCB4) ceramic aggregates, which denotes a larger amount of accessible voids. These results well agree with the water absorption values: $\approx$ 8.5% for the tile ceramic and $\approx$ 11.5% for the RCB recycled aggregates. Conversely, the low water absorption values were found for the natural aggregates (2.46% and 2.70% for limestone and siliceous sand, respectively). The lowest value among the recycled aggregates was obtained for the sanitaryware waste ($\approx$ 1.6%), which is attributed to the high compactness and smoothness of particles. Similarly, bigger

differences between the specific density of the saturated (ρ_{S_SAT}) and dry particles (ρ_{S_DRY}) were observed in the TCW and RCB recycled aggregates compared with the natural ones, which is also attributed to the larger amount of water in the accessible voids.

Table 3. Physical properties of aggregates

	Loose bulk density, g/m^3	Voids between particles, %	Relative density of dry particles[1], g/m^3	Specific density saturated particles[2], g/m^3	Specific density dry particles[3], g/m^3	Water absorption, wt.%
Siliceous	1.49	36.86	2.51	2.42	2.36	2.46
Limestone	1.50	40.94	2.73	2.61	2.54	2.70
TCW 2	1.15	40.10	2.30	2.08	1.92	8.55
TCW 4	1.21	38.89	2.37	2.14	1.98	8.46
RCB2	1.01	48.21	2.23	2.14	1.95	11.64
RCB4	1.05	46.15	2.25	2.16	1.95	11.43
CSW2	1.21	46.46	2.28	2.27	2.26	1.63
CSW4	1.25	45.17	2.31	2.29	2.28	1.58

[1] $\rho_r = \dfrac{W_{DRY}}{V_r}$ [2] $\rho_{S\_SAT} = \dfrac{W_{SAT}}{V_A}$ [3] $\rho_{S\_DRY} = \dfrac{W_{DRY}}{V_A}$

3.3 Alkali-activated TCWP mortars with natural and TCWA recycled aggregates: approach to optimum mix proportions

Mortars were developed according to the mix proportions described in Table 2 (Section 2.4) using TCWP as the precursor and a w/b ratio of 0.45. They were successfully prepared with natural aggregates. Fresh mortars presented good workability, and compaction by vibration into moulds was very easy. Hardened mortars yielded compressive strength values of 9.45 MPa and 34.22 MPa (after 3 curing days at 65°C) in the mortars prepared with the siliceous and the limestone aggregates, respectively. However, this mix proportion did not work when TCWA was used as the recycled aggregate as particles did not compact and agglomerate when vibrated into moulds. This behaviour was attributed to the high water absorption of the TCWA particles, which significantly reduced the water available for the compaction process. Thus the mix

proportions were adapted according to the physical properties of the recycled aggregates. The w/b ratio was increased to 0.50 and, in order to prevent the alkali-activating solution from being absorbed by aggregates and losing reaction capacity, ceramic particles were previously saturated with water before being mixed with the alkali-activated TCWP paste. Under these conditions, two different water/binder ratios were defined: total w'/b (where w' is the total amount of water added to the system), and the effective w/b ratio (where w is the total amount of water, minus that absorbed by aggregates, as defined in UNE EN 206-1). The new mix proportions used, together with the designation of samples, the total and effective water/binder ratios (the total ones indicated in parentheses, (w'/b)) and the sodium and silica content per kg of binder, are summarised in Table 4. The mix proportions previously used to prepare the mortars with natural aggregates were also included for comparison purposes (45/10/1.16-5). Designation was modified to indicate the aggregate type used (S-Siliceous; L-Limestone; TCW2 and TCW4) and the total water/binder ratio (w'/b) since all the mortars were prepared with the same alkali-activating solution. Thus 50(67) means an effective w/b ratio of 0.50 and a total (w'/b) ratio of 0.67. Under these conditions, fresh mortars were easily compacted by vibration into moulds.

Table 4. The mix proportions, effective and total w/b ratios for the alkali-activated TCW mortars

Designation	Aggregate	w/b Effective water	(w'/b) Total water	$[Na^+]$, $Mol.kg^{-1}$	SiO_2/Na_2O, Molar ratio	$Ca(OH)_2$, %	Na^+, mol. kg_{binder}^{-1}	SiO_2, mol. kg_{binder}^{-1}
45/10/1.16-5	Limestone Siliceous	0.45	0.45	10	1.16	5	4.50	2.62
50(67) - S 50(67) - L 50(67) -TCW2 50(67) –TCW4	Siliceous Limestone TCW2 TCW4	0.50	0.67	10	1.16	5	5.00	2.91

The compressive strengths of the alkali-activated TCW mortars prepared with natural and recycled aggregates, with a 0.50 effective w/b ratio, cured at 65ºC for 3, 7 and 28 days, and at 20ºC for 7, 28 and 90 days, are summarised in Figure 6. Good mechanical properties were generally obtained in the mortars cured at 65ºC for 7 days, and low strength values were

achieved in the samples cured at room temperature, whatever the curing time. This means that, regardless of the material used as the aggregate, thermal activation needs to be applied for the TCWP activation process to take place.

The mortars prepared with natural siliceous aggregates exhibited very poor mechanical properties, even when cured at 65ºC (lower than 3.5 MPa after 3 curing days). Thus their data are not plotted in Figure 6 as no significant compressive strength gain was observed. The samples prepared with limestone aggregates presented the best mechanical properties among those cured at room temperature. However, their strength reached a maximum after 7 curing days at 65ºC, and then slightly diminished (up to 28 days). The mechanical properties of the mortars that contained TCW did not vary significantly with curing time at room temperature, and progressively increased when cured at 65ºC. This improvement was more significant with the finest aggregate sample (TCW2), and 53 MPa and 42.5 MPa were achieved in the mortars prepared with TCW2 and TCW4 (28 days, 65ºC), respectively. Although the differences between these strength values are attributed mainly to the greater fineness of TCW2, they may also be influenced by grain packing effects.

INSERT FIGURE 6

3.4 Optimisation of dosage: mechanical strength target

The effective water of mixes was reduced to develop more sustainable mortars with lower sodium and silica contents, and to optimise the compressive strength values. Mix proportions were designed with an effective w/b ratio of 0.45, and aggregates were also saturated with water prior to the mixing process so that a total (w'/b) ratio of 0.63 was used. As the mechanical properties of the mortars prepared with siliceous aggregates (Section 3.3) were poor, they were not included in this part of the study. The aggregates used during the optimisation process were natural limestone sand and recycled TCW4, which presented similar particle size distributions.

The compressive strength values of the prepared mortars cured at 65ºC for 3, 7 and 28 days, and at 20ºC for 7, 28 and 90 days, are summarised in Figure 7.

The material used as the aggregate significantly influenced the mechanical properties of the mortars, and those prepared with limestone particles generally exhibited better mechanical properties than the mortars prepared with recycled TCW4. Aggregate type proved more influential at 20ºC, which agrees well with the previous results presented in Section 3.3. However, the limestone mortars cured at 65ºC obtained better compressive strength results at short curing times (3 and 7 days), and major strength loss occurred after 28 curing days. On the contrary, no reduction in the mechanical properties was observed in the mortars prepared with the TCW4 recycled aggregate.

INSERT FIGURE 7

3.5 Mechanical properties of the mortars developed by combining natural and TCW recycled aggregates

Natural aggregates (limestone and siliceous) were replaced with TCWA (0 to 100 wt.%) to analyse the influence of the different proportions on the mechanical properties of mortars. All the mortars were prepared by considering an effective w/b ratio of 0.45 (the mix proportions indicated in Table 2), and the water added to the recycled aggregates prior to the mixing process was determined according to their water absorption values. The compressive strength values and total (w'/b) ratios of the mortars prepared with the different natural/TCWA proportions, cured at 65ºC for 3 days, are presented in Figure 8. The mortars that contained only limestone aggregates achieved 32 MPa, whereas 10 MPa was the result for that prepared with siliceous particles. The mechanical strength of the mortars developed with 100 wt.% TCW recycled aggregates (TCW2 or TCW4) fell between the other values (≈23 MPa). Although the amount of water required to presaturate the TCW2 aggregate was larger than that used for

14

TCW4 (due to the larger specific surface of the former), both mortars presented similar compressive strength results after 3 curing days at 65ºC, no matter what their particle size was.

The mechanical properties of the mortars prepared with the siliceous aggregate progressively improved with TCW2 content, and the best results (≈23 MPa) were obtained in that prepared with 100 wt.% ceramic waste. On the contrary, an optimum proportion of the 'limestone/TCW4' combination was observed, and the mortars prepared with equal amounts of natural and recycled aggregates (50/50 wt.%) yielded the best compressive strength value (≈43 MPa).

INSERT FIGURE 8

3.6 Mechanical properties of the mortars developed with the red clay brick and sanitaryware ceramic waste aggregates.

The compressive strengths of the alkali-activated TCWP mortars developed with the natural and the different types of ceramic waste recycled aggregates, cured at 65ºC for 3 days, are plotted in Figure 9. An effective w/b ratio of 0.45 was used for all the prepared mortars (see the mix proportions in Table 2), and different amounts of water were added to aggregates, depending on their water absorption and particle size (the total w'/b ratio is indicated in parentheses). The main parameter that affected the compressive strength of the developed mortars was the material used as the recycled aggregate. Similar results were obtained for each ceramic material, independently of the particle size or the total (w'/b) ratio of the mix. Conversely, huge differences were observed between natural aggregates; whereas the mortars prepared with the limestone particles exhibited the best mechanical properties after 3 curing days, the corresponding mortar with the siliceous particles gave the lowest compressive strength value.

INSERT FIGURE 9

3.7 Microscopic studies of the mortar samples

Optical microscopy images of the mortars developed with an effective w/b ratio of 0.45, prepared with TCW4, the limestone aggregate and a combination of both (50 wt.% each), cured at 65ºC for 28 days, are presented in Figures 10-12. All the prepared mortars presented a homogeneous distribution of aggregates, with the binder completely surrounding particles, whatever aggregate type was used. Whitened areas in the mortar prepared by combining the natural and recycled aggregates were observed (see Fig. 12 a), probably due to efflorescence formation.

INSERT FIGURES 10 TO 12

The backscattered SEM micrographs and EDS analyses of these mortars are presented in Figures 13-15. The EDS results corroborated the chemical and mineralogical composition of TCW, as previously reported in [17], where silicon and aluminium were the main elements identified in the alkali-activated matrix and within TCW aggregates. Calcium was not only detected in limestone particles, but also within the binding matrix, as $Ca(OH)_2$ was added to the mix (5 wt.%) to activate the binding reaction, and 5.77% of CaO was present in TCW. High Ca concentrations clearly denoted presence of limestone aggregates, whereas unreacted TCW particles were identified by higher Si concentrations. No reaction products were clearly distinguished in the transition zone between the recycled aggregates and the binding matrix. However, the fact that ceramic waste was successfully used as a precursor in the alkali-activated system suggests that some reaction may occur in the interfacial transition zone between the TCWA particles and the binding paste. This would improve adherence and, consequently, behaviour in compressive strength terms.

Sodium was uniformly distributed along the binding matrix in the mortars prepared only with the TCWA recycled aggregate (Fig. 13b). However, higher sodium concentrations were observed to surround the limestone particles in the mortars prepared only with the limestone aggregates

(Fig. 14b), and areas of the binding matrix with a low sodium concentration were identified in the mortars developed with the limestone/TCW4 combination (Fig. 15b). Finally, no cracking was clearly observed in any of the prepared mortars, on the surface of specimens, or in the interfacial transition zone between aggregates and the paste.

INSERT FIGURES 13 TO 15

The interfacial transition zone (ITZ) between the limestone aggregate and the binding paste was further analysed by EDS to investigate chemical composition evolution. Figure 16 illustrates relative amounts of Ca, Na and Si along 50 and 20 μm lengths, with analyses performed every 0.425 and 0.249 μm, respectively. As observed, the relative amount of Ca progressively increased along the ITZ (10 and 6 μm in Fig. 16a and 16b, respectively), from the binding matrix to the limestone particles

INSERT FIGURE 16

In the samples that contained the limestone aggregate (100% or 50%), salt efflorescence arose when the plastic film covering the specimen was removed and the material was exposed to laboratory conditions. This behaviour was not observed for the mortars prepared with only the recycled aggregates. The X-ray diffraction pattern of the efflorescence formed in these mortars is plotted in Figure 17. The analysis denoted presence of hydrated sodium carbonate thermonatrite ($Na_2CO_3 \cdot H_2O$, PDFcard080448) and calcite ($CaCO_3$, PDFcard050586) as the main crystalline phases, and quartz (SiO_2, PDFcard331161) also appeared given their presence in TCW. Small amounts of hydrated calcium carbosilicate scawtite ($Ca_7(Si_6O_{18})CO_3 \cdot 2H_2O$, PDFcard310261) and hydrated sodium and calcium carbonate gaylussite ($Na_2Ca(CO_3)_2 \cdot 5H_2O$, PDFcard210343) were also identified.

INSERT FIGURE 17

3.8 Dissolution tests of the TCW and limestone aggregates

The interaction of the limestone and TCW aggregates with the binding paste was further investigated by running dissolution tests of the particles in the alkali-activating solution. The as-received limestone aggregates presented a low porosity surface (Fig. 18a), composed of grouped irregular particles (Fig. 18b). As shown in Figure 19, after being immersed in the alkali-activating solution for 7 days at 65ºC, the texture of the particles significantly changed (Fig. 19a) and the surface porosity notably increased (Fig. 19b), which denotes the occurrence of dissolution reactions.

INSERT FIGURES 18 and 19

The original TCW aggregates exhibited a highly compact matrix that contained approximately 1-µm pores (Fig. 20), whose rounded shape was attributed to the partial fusion of the ceramic material during its production process. As Figure 21 shows, the texture of the TCW particles vastly changed after immersion in the activating solution for 7 days (65ºC): the material was partially dissolved, the original rounded pores could not be clearly distinguished, and crystalline particles appeared (probably those previously identified by XRD in the TCW raw material; i.e. quartz, mullite, albite or diopside, see Section 2.2). These changes clearly denote some dissolution of the TCW aggregates by the activating solution under the studied conditions.

INSERT FIGURES 20 and 21

4   Discussion

The mortars developed at 65ºC exhibited compressive strength values within the 25-40 MPa range after 7 curing days, whereas reduced mechanical properties (5 to 12 MPa) were obtained in those cured at 20ºC for 28 days. Thus a moderate curing temperature is required to

accelerate the alkali-activation of TCW, which implies that the developed mortars could be used only in prefabricated applications. However, previous studies into the influence of different sources of calcium (e.g., calcium aluminate cement or calcium hydroxide) on the mechanical properties and microstructure of alkali-activated blast furnace slag [18] or porcelain stoneware tiles [10] have shown a positive effect. Although it was not the purpose of the present study, this would be an extremely interesting research line to be explored since activating the material at room temperature would considerably extend the field of applications in which the TCW alkali-activated samples could be used.

The mechanical properties of the developed TCWP alkali-activated mortars generally improved with curing time and temperature (Sections 3.3 and 3.4), which agrees with previous studies on the development of new low CO_2 binders by the alkali activation of other ceramic materials [9,10]. The development of mechanical strength with curing time probably occurs due to changes in the chemical composition of the binding gel, as explained in [1]. The mechanical behaviour observed herein also coincides with that previously reported by Criado et al. [19], who observed a lesser extent of the reaction process and mechanical properties, together with the formation of sodium carbonate salts, in open cured alkali-activated fly ash samples compared to those cured at 85ºC. It is generally accepted that hydrothermal curing at temperatures above 65ºC improves compressive strength results and reduces efflorescence formation, which are attributed to the greater extent of geopolymerisation reactions [20].

Huge differences were observed between the mechanical properties of the mortars developed with the limestone and siliceous aggregate (Fig. 9). The mortars prepared with siliceous particles displayed poor mechanical properties, even when temperature was applied to cure samples. Contrarily, those prepared with limestone particles exhibited the best mechanical properties for the mortars cured at room temperature. The compressive strength of the limestone mortars reached a maximum when cured at 65ºC, but then decreased (Sections 3.3 and 3.4). Differences between the mechanical properties of the mortars prepared with the siliceous and limestone aggregates were attributed mainly to a different interaction between

19

aggregates and the binding matrix. As previously explained by Giganto and Moraño [21], siliceous particles generally present poorer mechanical and chemical adherence with the binding paste. The rougher and more porous surface generally presented by limestone aggregates, compared with that of siliceous particles, increases the contact surface with the binding paste. According to [21], fine limestone particles are not totally inert when they come into contact with cement, which contrasts with the high stability of siliceous particles (quartz). The results obtained for the limestone mortars are in line with those formerly reported by Puertas et al. [22] for sodium silicate alkali-activated slag mortars prepared with calcareous aggregates. These authors observed that the partial dissolution of aggregates, and the diffusion of calcium from these particles towards the binding matrix, conferred cohesion to the aggregate-paste interface.

The interaction of the limestone aggregate with the binding gel may also influence the composition of the gel formed during the alkali activation process, which would be responsible for the different sodium concentrations observed in the SEM analyses in the mortars that contained the limestone aggregate (100% or combined with TCW4, see Section 3.7). As reported by Provis et al. [23], the nanostructure of high-calcium alkali-activated materials (blast furnace slag) is formed mainly by a calcium aluminosilicate hydrate (C-A-S-H) gel, whereas low-calcium systems (i.e. metakaolin, fly ash) present a highly crosslinked sodium aluminosilicate hydrate (N-A-S-H) gel. Bernal et al. [24] also observed how the activation of fly ash/slag blends resulted in different binder gel types (N-A-S-H and C-A-S-H). The co-precipitation of these two gels [1] gives a complex mix of both, which may interact: C-A-S-H (whose composition includes sodium) and (N,C)-A-S-H (N-A-S-H with a high calcium content). As summarised by Garcia-Lodeiro et al. [1], the formation of C-A-S-H over N-A-S-H gel is favoured over time if calcium concentrations and pH values are high (above 12). In the present study, the compressive strength of the mortars that contained the limestone aggregate, which were cured at 65ºC, slightly reduced with curing time, whereas the mechanical properties of that prepared with the TCWA aggregates progressively increased during the same curing period (3 to 28 days at 65ºC). According to the aforementioned studies [1,22-24], the calcium ions in the limestone-

containing mortars migrate towards the binding matrix to lead to a N-A-S-H to (N,C)-A-S-H gel transformation, which results in a release of sodium ions. With short curing times, this process enhances the interfacial transition zone and improves compressive strength. However for longer curing periods (28 days at 65ºC), a slight reduction of the mechanical properties of the mortars was observed (see Figs. 6 and 7). This behaviour could be attributed to several factors: a) partial dissolution of the aggregate surface, which would weaken the adherence between the limestone aggregate and the TCWP alkali-activated binding matrix; b) partial crystallisation of the hydration products; c) further efflorescence formation due to increasing amounts of free Na^+ ions.

According to [1], the compositional and structural changes observed in N-A-S-H gels do not significantly affect the material's strength. However, the evolution of N-A-S-H to (N,C)-A-S-H facilitates sodium ions to leach out of the binding matrix and efflorescence formation (as described in Section 3.7). As reported in [25,26], the main role of alkalis during the alkali-activation process is to generate high pH conditions for precursor dissolution and, once the new gel has been formed, to remain weakly bonded in the nanostructure and to balance the newly formed gel. Studies performed on alkali-activated metakaolin and fly ash have also confirmed that almost all alkalis can be simply leached out without it significantly affecting the mechanical properties or the material's gel structure [26]. Thus presence of limestone aggregates influences the newly formed gel's composition, and results in a larger amount of free alkalis, which leads to the formation of the observed efflorescence. According to Allahverdi et al. [27], efflorescence consists in the formation of deposits of salts on the material's surface, caused by the evaporation of the soluble constituents previously dissolved by water. Although presence of efflorescence is initially considered an aesthetic defect and is not necessarily linked to binding matrix degradation, continuous progression can generate internal stresses that affect the material's integrity. Upon strong leaching of alkalis, depassivation of the steel bars embedded in the reinforced concrete could also happen. In the present study, efflorescence arose when the plastic film protection on mortars samples was removed, and specimens came into contact with the laboratory atmosphere (RH ≈40%) as the water contained in mortars evaporated and

diffusion of CO_2 into mortars was allowed. According to Provis et al. [23] and to Bernal [28], intermediate humidity conditions are required to enable the uptake of CO_2 from the atmosphere as saturation of pores with moisture under very high RH conditions hinders CO_2 diffusivity. Moreover, carbonation process speed also slows down under low humidity conditions due to a difficult CO_2 hydration to form carbonic acid. Some of the mineralogical phases identified in the XRD pattern plotted in Figure 17 (thermonatrite, scawtite and gaylussite) can take place as a result of the diffusion of sodium and calcium ions through the capillary network, and their interaction with atmospheric CO_2. Thermonatrite $Na_2CO_3 \cdot H_2O$ formation has also been reported by Skvára et al. [29] in the efflorescence generated in low calcium fly ash geopolymers, and Bernal et al. [24] identified the formations of natron ($Na_2CO_3 \cdot 10H_2O$), nahcolite ($NaHCO_3$) and gaylussite ($Na_2Ca(CO_3)_2 \cdot 5H_2O$) in carbonated alkali-activated slag/fly ash samples. Palacios and Puertas [30] identified natron and calcium carbonate polymorphs (calcite, vaterite and aragonite) under accelerated conditions in activated blast furnace slag binders. These phases may also be partially responsible for the slight reduction in the mechanical properties observed in the limestone-containing mortars cured at 65ºC for 28 days.

The material used as an aggregate proved to be an essential parameter when designing alkali-activated TCW mortars (Section 3.6). With the recycled ceramic aggregates used herein, the best results were obtained for the RCB waste. This is attributed to the material's higher porosity, which allows the precipitation of the binding gel into the pore network. In contrast, the CSW mortars displayed the poorest performance because, in this case, the material's low open porosity hinders the gel from penetrating into pores.

5 Conclusions

This research has demonstrated that mortars with high tile ceramic waste (TCW) contents, used as a recycled aggregate and a precursor, can offer a potential reuse application for a waste material produced in vast amounts. The conclusions drawn according to the results of this paper are:

- The lower density and higher water absorption values of the TCWA recycled aggregates, compared with the natural limestone and siliceous aggregates, mean that it is necessary to adapt the preparation process of mortars by saturating recycled aggregates with water before being mixed with the alkali-activated TCWP binding paste.

- The compressive strength results of the alkali-activated TCWP mortars cured at 65ºC for 3 days depend mainly on the type of material used as the recycled aggregate (TCWA, RCB, CSW), and vary slightly with particle size or the total (w'/b) ratio of the mix. The RCB mortars, whose recycled aggregate shows the highest water absorption, obtain the best results, whereas the lowest strength development is seen for the aggregate with the lowest water absorption values (CSW).

- The use of natural or TCW aggregates greatly influences the mechanical properties of the alkali-activated TCW mortars. The mortars that contain only limestone aggregates obtain more than 30 MPa compressive strength (3 days, 65ºC), and strength improves by adding TCW4, up to an optimum percentage of 50 wt.% (≈43 MPa). The mortars prepared only with siliceous particles present reduced mechanical properties (10 MPa, 3 days 65ºC), which progressively increase with higher TCW2 contents, up to the 23 MPa exhibited by that prepared only with this recycled aggregate.

- Limestone particles interact with the binding matrix. In the mortars cured at room temperature, the diffusion of calcium from the limestone aggregates towards the binding gel confers cohesion, which improves the compressive strength results. Conversely, the higher kinetics of the process in the mortars cured at 65°C reduces the mortar mechanical properties for curing times longer than 7 days.

- Efflorescence arises in the mortars that contain the limestone aggregate given their interaction with the binding matrix, which results in a larger amount of free alkalis.

References

[1] I. García-Lodeiro, A. Palomo, A. Fernández-Jiménez, An overview of the chemistry of alkali-activated cement-based binders, in: F. Pacheco-Torgal, J. Labrincha, C. Leonelli, A. Palomo, P. Chindaprasit (Eds.), Handbook of Alkali-Activated Cements, Mortars and Concretes, Woodhead Publishing; 1st edition, United Kingdom, 2014, pp. 19–47.

[2] F. Pacheco-Torgal, Introduction fo Handbook of Alkali-activated Cements, Mortars and Concretes, in: F. Pacheco-Torgal, J. Labrincha, C. Leonelli, A. Palomo, P. Chindaprasit (Eds.), Handbook of Alkali-Activated Cements, Mortars and Concretes, Woodhead Publishing; 1st edition, United Kingdom, 2014, pp. 1–18.

[3] C. Shi, a. F. Jiménez, A. Palomo, New cements for the 21st century: The pursuit of an alternative to Portland cement, Cem. Concr. Res. 41 (2011) 750–763. doi:10.1016/j.cemconres.2011.03.016.

[4] A. Mellado, C. Catalán, N. Bouzón, M. V. Borrachero, J.M. Monzó, J. Payá, Carbon footprint of geopolymeric mortar: study of the contribution of the alkaline activating solution and assessment of an alternative route, RSC Adv. 4 (2014) 23846–23852. doi:10.1039/c4ra03375b.

[5] M. Behera, S.K. Bhattacharyya, A.K. Minocha, R. Deoliya, S. Maiti, Recycled aggregate from C&D waste & its use in concrete - A breakthrough towards sustainability in construction sector: A review, Constr. Build. Mater. 68 (2014) 501–516. doi:10.1016/j.conbuildmat.2014.07.003.

[6] J. Payá, J. Monzó, M.V. Borrachero, M.M. Tashima, Reuse of aluminosilicate industrial waste materials in the production of alkali-activated concrete binders, in: F. Pacheco-Torgal, J. Labrincha, C. Leonelli, A. Palomo, P. Chindaprasit (Eds.), Handbook of Alkali-Activated Cements, Mortars and Concretes, Woodhead Publishing; 1st edition, United Kingdom, 2014, pp. 487–514.

[7] N. Marjanovic, M. Komljenovic, Z. Bascarevic, V. Nikolic, R. Petrovic, Physical-mechanical and microstructural properties of alkali-activated fly ash-blast furnace slag blends, Ceram. Int. 41 (2015) 1421–1435. doi:10.1016/j.ceramint.2014.09.075.

[8] A. Pereira, J.L. Akasaki, J.L.P. Melges, M.M. Tashima, L. Soriano, M. V. Borrachero, et al., Mechanical and durability properties of alkali-activated mortar based on sugarcane bagasse ash and blast furnace slag, Ceram. Int. (2015) 1–13. doi:10.1016/j.ceramint.2015.07.001.

[9] L. Reig, M.M. Tashima, M. V. Borrachero, J. Monzó, C.R. Cheeseman, J. Payá, Properties and microstructure of alkali-activated red clay brick waste, Constr. Build. Mater. 43 (2013) 98–106. doi:10.1016/j.conbuildmat.2013.01.031.

[10] L. Reig, L. Soriano, M.V. Borrachero, J. Monzó, J. Payá, Influence of the activator concentration and calcium hydroxide addition on the properties of alkali-activated porcelain stoneware, Constr. Build. Mater. 63 (2014) 214–222. doi:10.1016/j.conbuildmat.2014.04.023.

[11] R. V. Silva, J. De Brito, R.K. Dhir, Tensile strength behaviour of recycled aggregate concrete, Constr. Build. Mater. 83 (2015) 108–118. doi:10.1016/j.conbuildmat.2015.03.034.

[12] M. Elchalakani, E. Elgaali, Sustainable concrete made of construction and demolition wastes using recycled wastewater in the UAE, J. Adv. Concr. Technol. 10 (2012) 110-125. doi: 10.3151/jact.10.110.

[13] A.V. Alves, T.F. Vieira, J. De Brito, J.R. Correia, Mechanical properties of structural concrete with fine recycled ceramic aggregates, Constr. Build. Mater. 64 (2014) 103–113. doi:10.1016/j.conbuildmat.2014.04.037.

[14] C. Medina, A. Juan, M. Frías, M. I. Sánchez de Rojas, J. M. Morán, M. I. Guerra, Characterization of concrete made with recycled aggregate from ceramic sanitary ware, Mater. Construcción 61 (304) (2011) 533-546. doi: 10.3989/mc.2011.59710.

[15] Federación española de gestores de residuos de construcción y demolición (FERCD). Informe de producción y gestión de los residuos de construcción y demolición (RCD) en España, periodo 2009-2013. http://www.rcdasociacion.es/images/documents/INFORME%20RCD%202015%20(2).pdf, 2015 (accessed March 2017)

[16] D. Stock, World production and consumption of ceramic tiles, Tile Today 85 (2014) 54–62.

[17] M.A. Mas, J. Monzó, J. Payá, L. Reig, M.V. Borrachero, Ceramic tiles waste as replacement material in Portland cement, Adv. Cem. Res. (2015) 1–12. doi: 10.1680/adcr.15.00021.

[18] K. Arbi, A. Palomo, A. Fernández-Jiménez, Alkali-activated blends of calcium aluminate cement and slag/diatomite, Ceram. Int. 39 (2013) 9237-9245.

[19] M. Criado, A. Palomo, A, Fernández-Jiménez, Alkali activation of fly ashes. Part 1: Effect of curing conditions on the carbonation of the reaction products, Fuel 84 (16) (2005) 2048-2054.

[20] J. Temuujin, A. van Riessen, R. Williams, Influence of calcium compounds on the mechanical properties of fly ash geopolymer pastes, J. Hazard. Mater. 167 (1-3) (2009) 82-88.

[21] J. Giganto, A.J. Moraño, Árido calizo 'versus' árido silíceo. I Congreso Nacional de Áridos, Zaragoza. Fueyo Editores (2006) 35-37.

[22] F. Puertas, M. Palacios, A. Gil-Maroto, T. Vázquez, Alkali-aggregate behaviour of alkali-activated slag mortars: Effect of aggregate type, Cem. Concr. Compos. 31 (2009) 277–284. doi:10.1016/j.cemconcomp.2009.02.008.

[23] J.L. Provis, A. Palomo, C. Shi, Advances in understanding alkali-activated materials, Cem. Concr. Res. 78 (2015) 110-125. doi:10.1016/j.cemconres.2015.04.013.

[24] S.A. Bernal, J.L. Provis, B. Walkley, R. San Nicolas, J.D. Gehman, D.G. Brice, et al., Gel nanostructure in alkali-activated binders based on slag and fly ash, and effects of accelerated carbonation, Cem. Concr. Res. 53 (2013) 127–144. doi:10.1016/j.cemconres.2013.06.007.

[25] P. Duxson, G.C. Lukey, F. Separovic, J.S.J. van Deventer, Effects of alkali cations on aluminium incorporation in geopolymeric gels, Ind. Eng. Chem. Res. 44 (4) (2005) 832-839. doi: 10.1021/ie0494216.

[26] F. Škvára, V. Šmilauer, P. Hlaváček, L. Kopecký, Z. Cílová, A weak alkali bond in (N, K)–A–S–H gels: evidence from leaching and modeling, Ceram-Silikaty 56 (4) (2012) 374-382.

[27] A. Allahverdi, E. Najafi-Kani, K.M.A. Hossain, M. Lachemi, Methods to control efflorescence in alkali-activated cement-based materials, in: F. Pacheco-Torgal, J. Labrincha, C. Leonelli, A. Palomo, P. Chindaprasit (Eds.), Handbook of Alkali-Activated Cements, Mortars and Concretes, Woodhead Publishing; 1st edition, United Kingdom, 2014, pp. 463–483.

[28] S.A. Bernal, The resistance of alkali-activated cement-based binders to carbonation, in: F. Pacheco-Torgal, J. Labrincha, C. Leonelli, A. Palomo, P. Chindaprasit (Eds.), Handbook of Alkali-Activated Cements, Mortars and Concretes, Woodhead Publishing; 1st edition, United Kingdom, 2014, pp. 319–332.

[29] F. Skvára, L. Kopecký, V. Smilauer, Z. Bittnar, Material and structural characterization of alkali activated low-calcium brown coal fly ash, J. Hazard. Mater. 168 (2-3) (2009) 711-720.

[30] M. Palacios, F. Puertas, Effect of carbonation on alkali-activated slag paste, J. Am. Ceram. Soc. 89 (2006) 3211–3221. doi:10.1111/j.1551-2916.2006.01214.x.

Fig. 1. Ceramic waste provided by ceramic tiles companies.
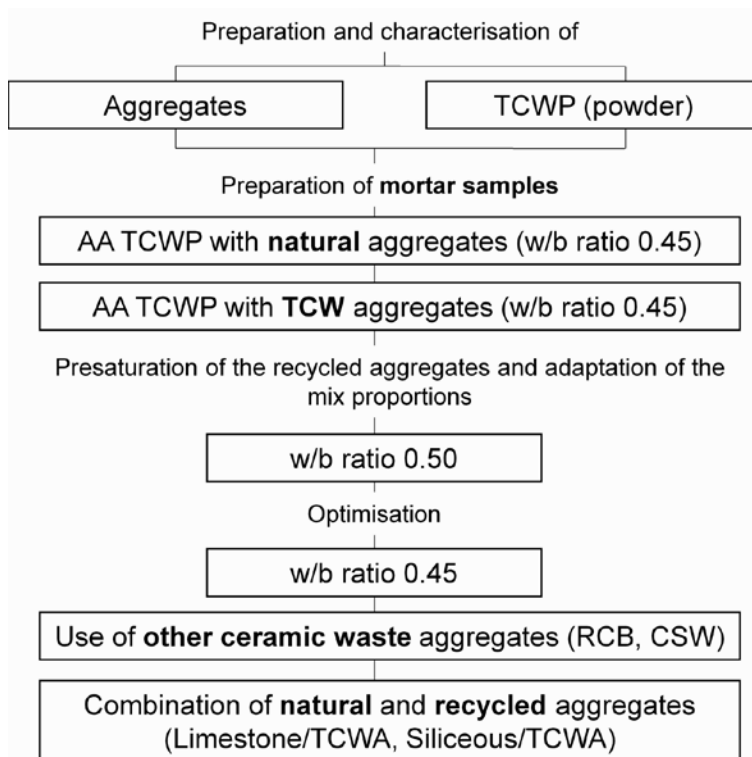
Fig. 2. Experimental flow chart of the alkali-activated TCW mortars with natural and recycled aggregates.
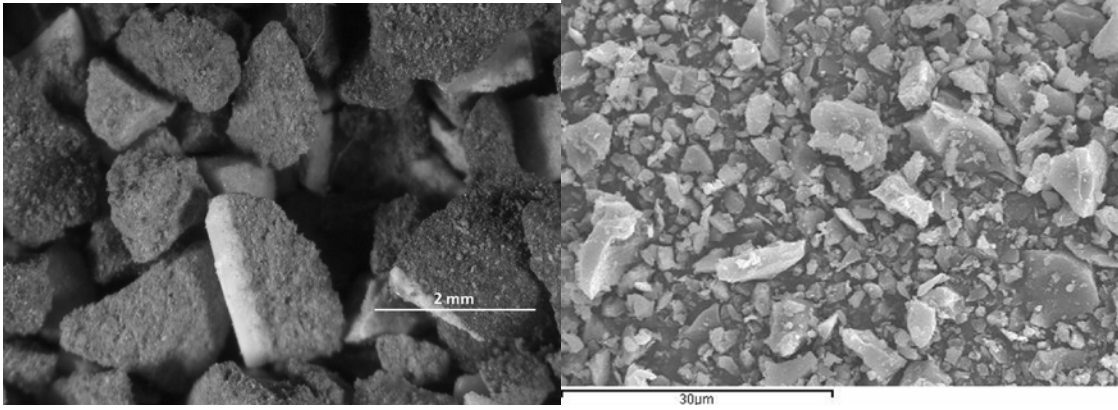
Fig. 3. Images of the TCW samples: a) Optical, crushed material; b) SEM, milled material (TCWP).
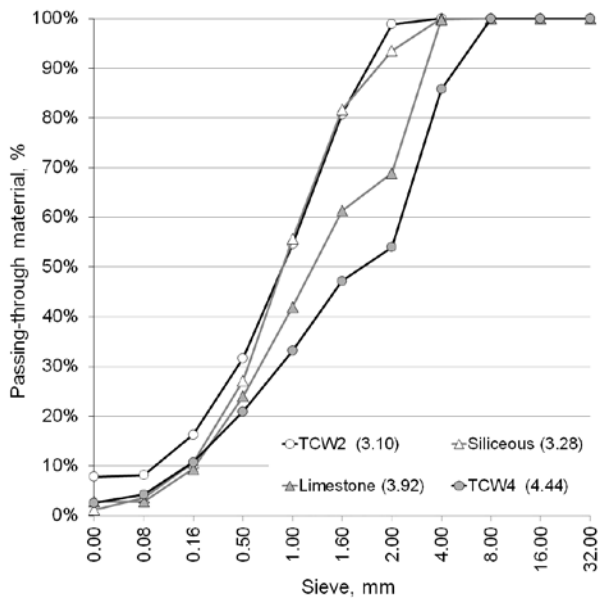
Fig. 4. Granulometric distribution of natural and TCW recycled aggregates. Fineness modulus indicated in parentheses.
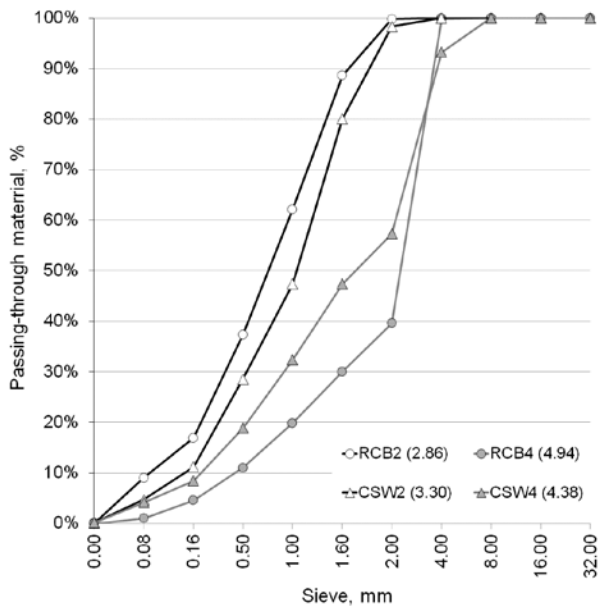
Fig. 5. Granulometric distribution of the red clay brick (RCB2 and RCB4) and sanitary ware (CSW2 and CSW4) recycled aggregates. Fineness modulus indicated in parentheses.
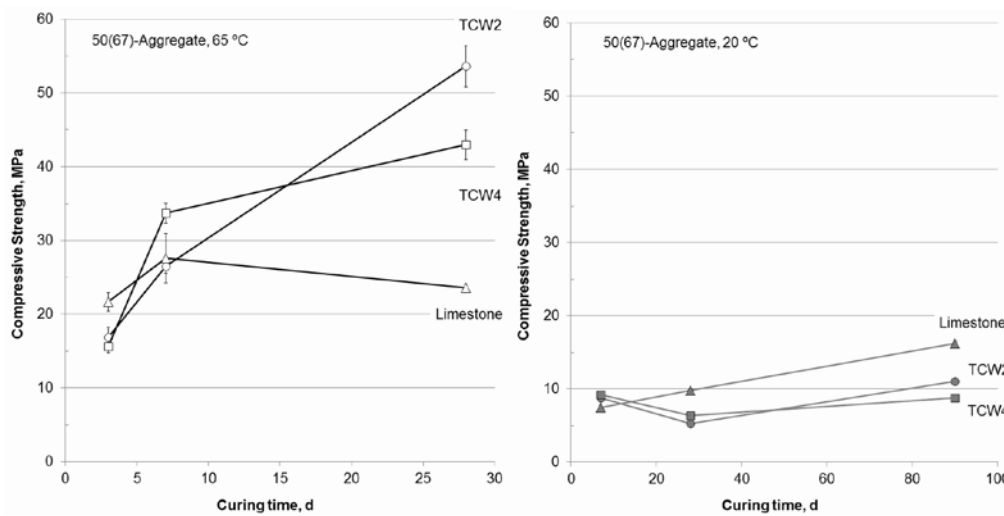
Fig. 6. Compressive strength developments of the alkali-activated TCWP 50(67) mortars: a) *cured at 65ºC; b) cured at 20ºC.*
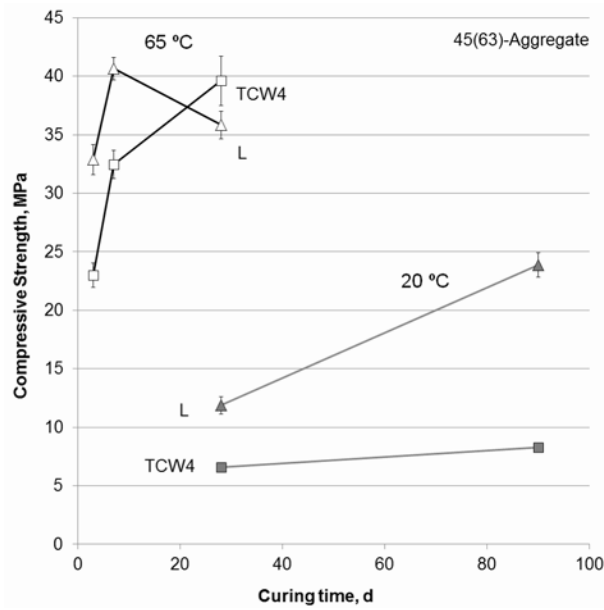
Fig. 7. Compressive strength of the alkali-activated TCWP 45(63) mortars cured at 65⁰C and 20⁰C with the limestone (L) and TCW4 aggregates.
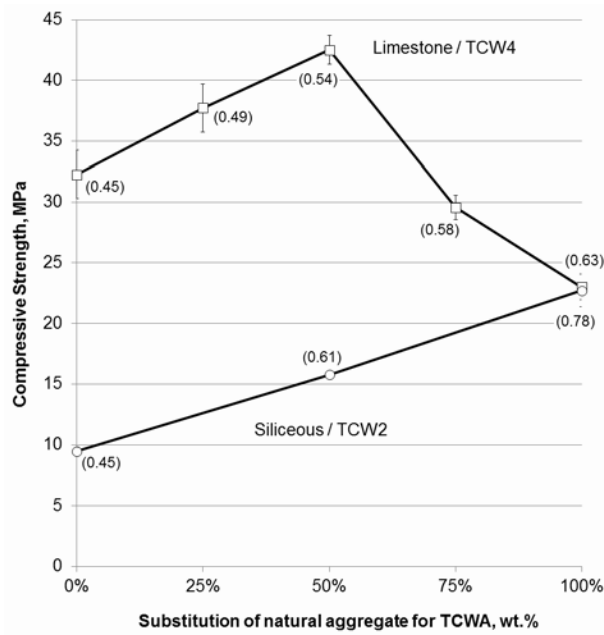
Fig. 8. Compressive strength of the mortars prepared with different natural/TCWA ratios, cured at 65⁰C for 3 days. Total (w'/b) ratio in parentheses; effective w/b ratio of 0.45.
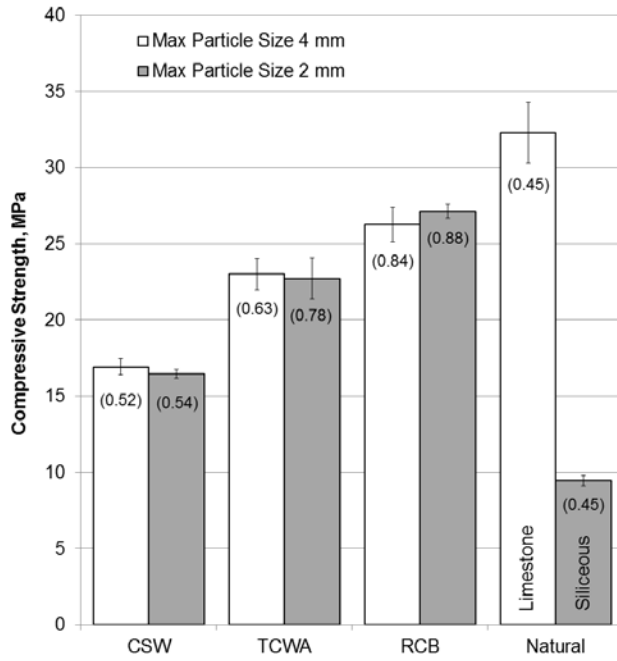
Fig. 9. Compressive strength of the mortars prepared with the natural and different types of ceramic recycled aggregates, cured at 65ºC for 3 days. Total (w'/b) ratio in parentheses.
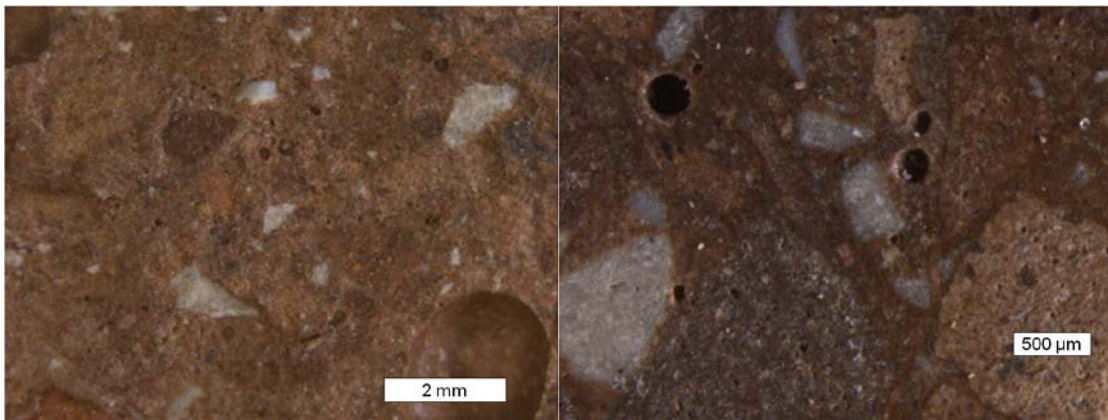
Fig. 10. Optical microscopy images of the alkali-activated mortar prepared with TCW4, cured at 65ºC for 28 d: a) fresh surface; b) polished surface.
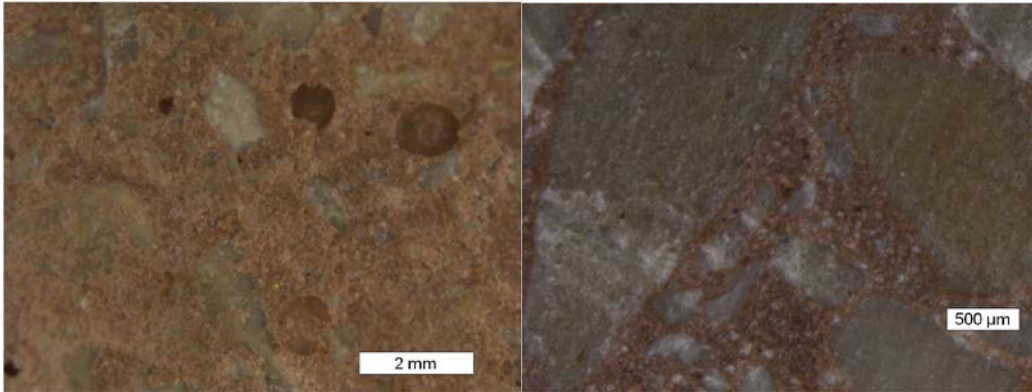
Fig. 11. Optical microscopy images of the alkali-activated mortar prepared with limestone aggregate, cured at 65ºC for 28 d: a) fresh surface; b) polished surface.
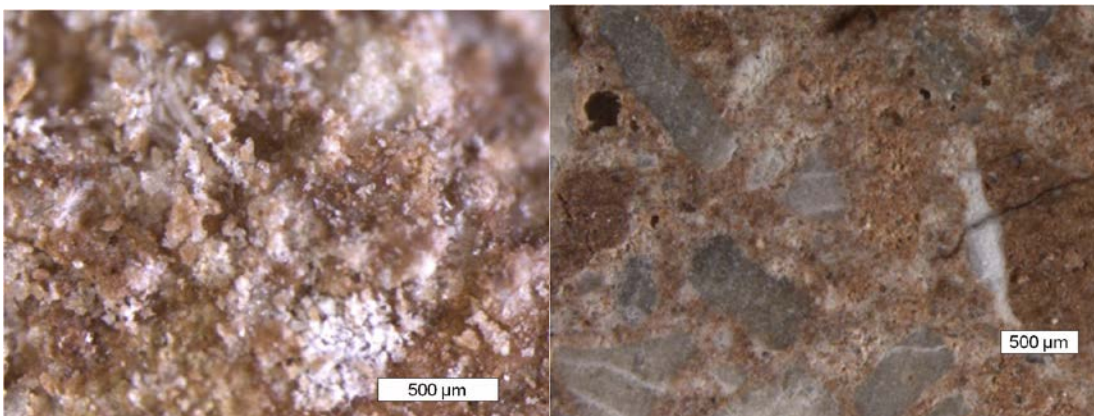
Fig. 12. Optical microscopy images of the alkali-activated mortar prepared with the 50 wt.% limestone/TCW4 combination, cured at 65ºC for 28 d: a) fresh surface; b) polished surface.
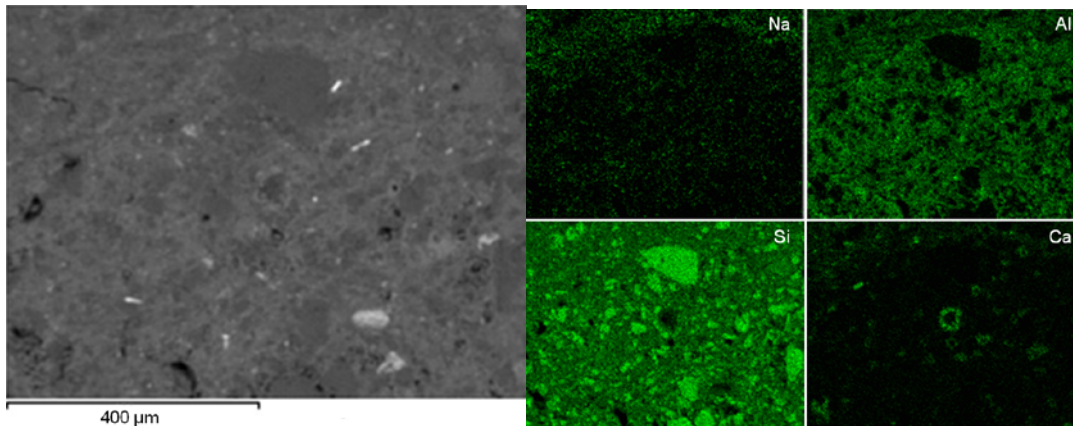
Fig. 13. SEM analyses of the alkali-activated mortar prepared with the TCWA recycled aggregate, cured at 65ºC for 28 d: a) Backscattered SEM image; b) Si, Al, Ca and Na distribution determined by EDS.
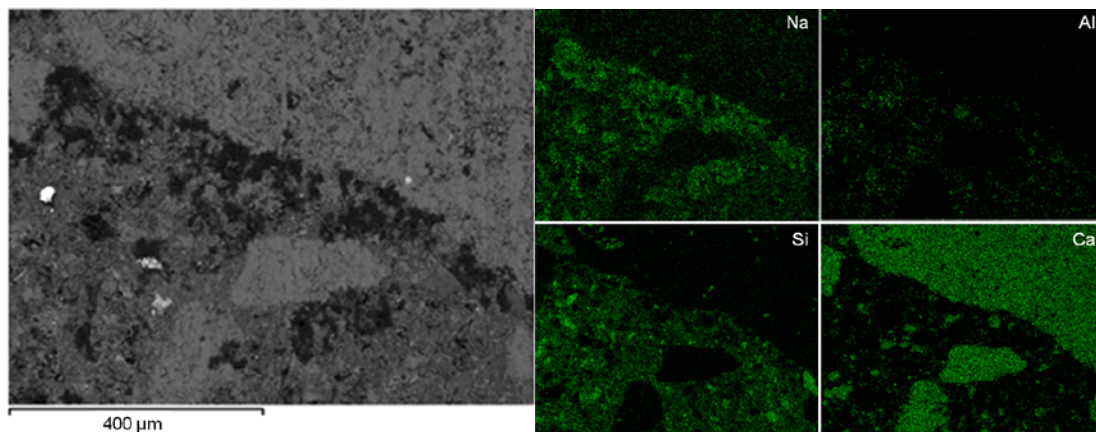
Fig. 14. SEM analyses of the alkali-activated mortar prepared with the limestone aggregate, cured at 65ºC for 28 d: a) Backscattered SEM image; b) Si, Al, Ca and Na distribution determined by EDS.
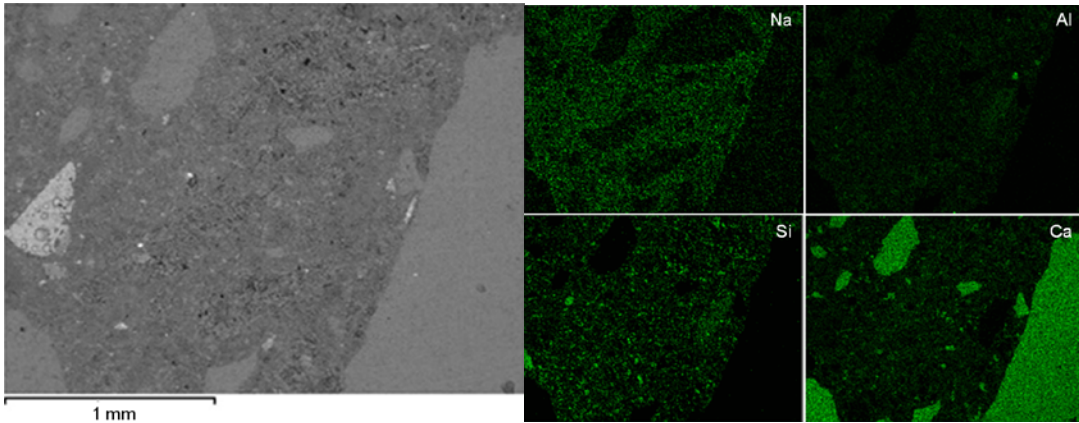
Fig. 15. SEM analyses of the alkali-activated mortar prepared with the 50 wt.% limestone/TCW4 combination, cured at 65ºC for 28 d: a) Backscattered SEM image; b) Si, Al, Ca and Na distribution determined by EDS.
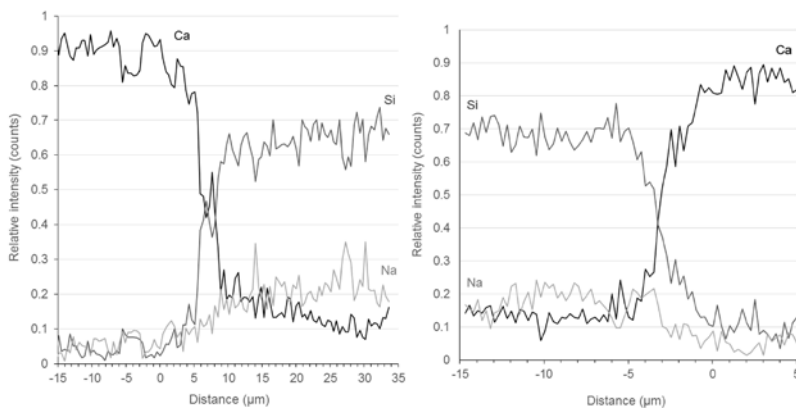
Fig. 16. Variation of Ca, Na and Si along the interfacial transition zone between the limestone aggregates and the binding paste: a) ITZ of a 10 μm length; b) ITZ of a 6 μm length.
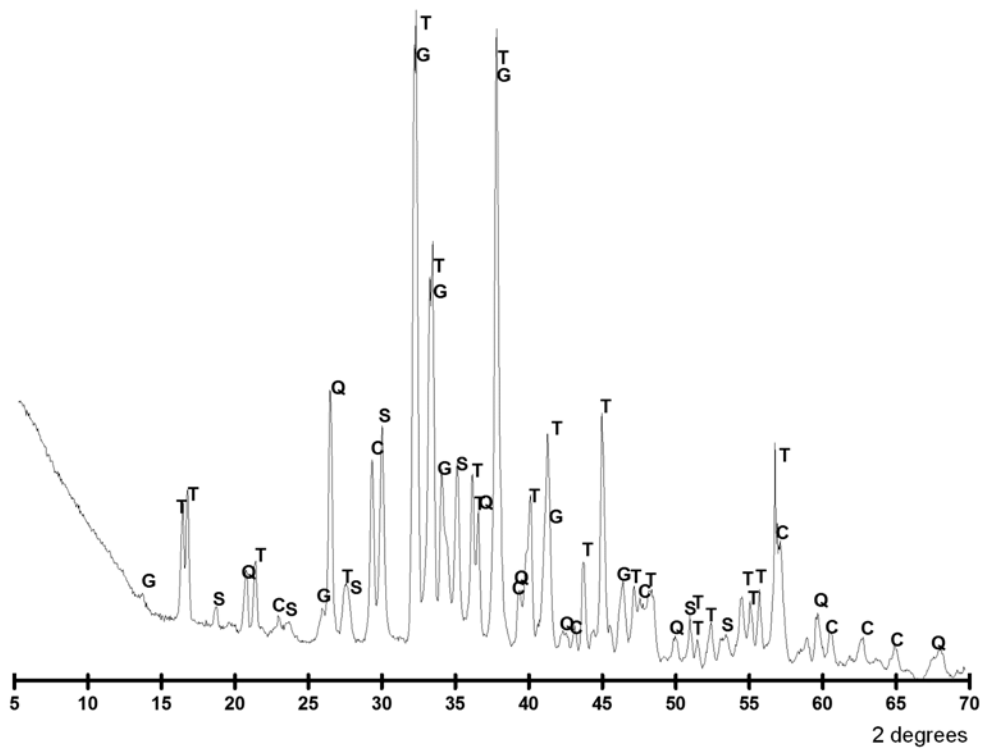
Fig. 17. The X-ray diffractogram for the salts that arose in the limestone aggregate-containing mortar, cured at 20ºC for 28 days. T = thermonatrite ($Na_2CO_3 \cdot H_2O$); C = calcite ($CaCO_3$); Q = quartz (SiO_2); S = scawtite ($Ca_7(Si_6O_{18})CO_3 \cdot 2H_2O$); G = gaylussite ($Na_2Ca(CO_3)_2 \cdot 5H_2O$).
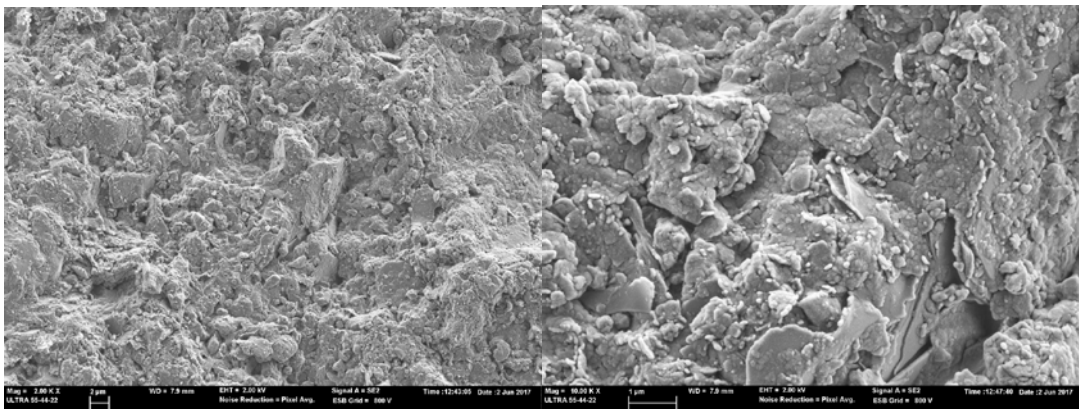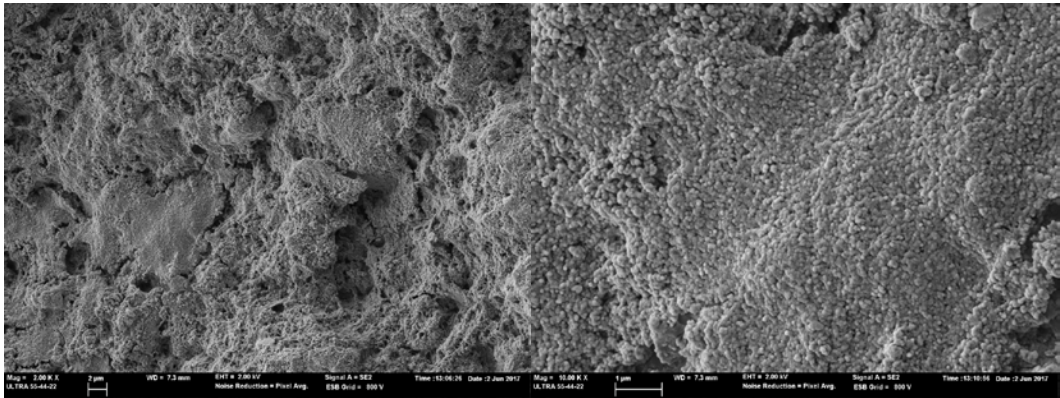

Fig. 18. SEM micrographs of the limestone aggregates, as received: a) General view; b) Magnification.

Fig 19. SEM micrographs of the limestone aggregates after immersion in the alkali-activating solution for 7 days at 65⁰C: a) General view; b) Magnification.
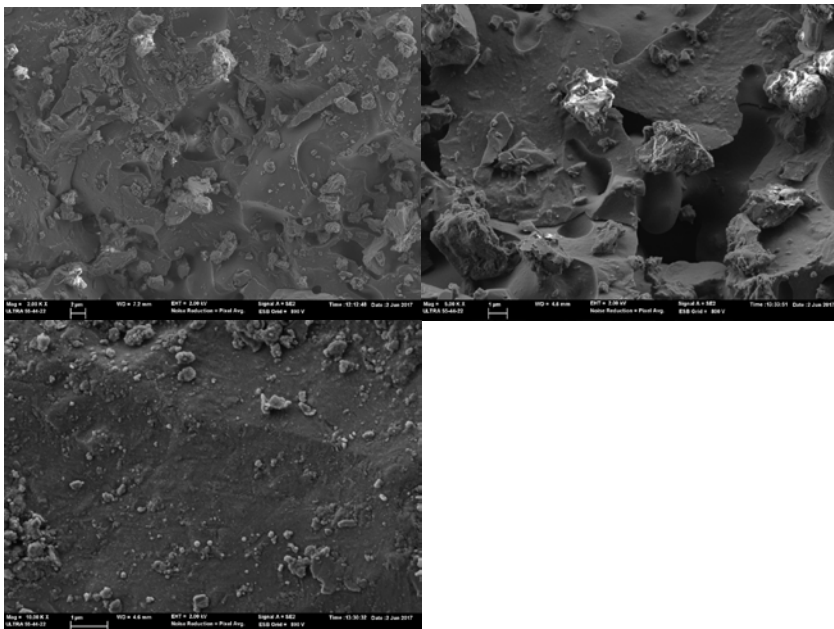

Fig 20. SEM micrographs of the TCW aggregates, as received: a) General view; b) Pore magnification; c) Solid phase magnification.
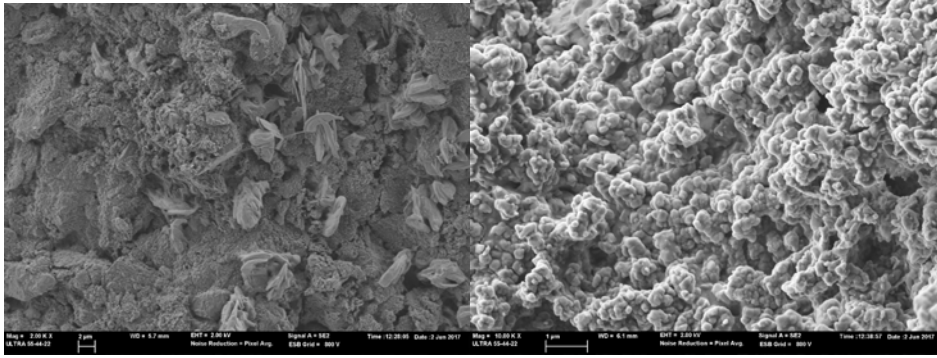
Fig. 21. SEM micrographs of the TCW aggregates after immersion in the alkali-activating

solution for 7 days at 65ºC: a) General view; b) Solid phase magnification.

TABLES

Table 1. Physical properties of the ceramic waste aggregates

Table 2. Mix proportions for the alkali-activated TCW mortars

Table 3. Physical properties of aggregates

Table 4. The mix proportions, effective and total w/b ratios for the alkali-activated TCW mortars